

Reliability Assessment of Nanoscale System on Chip Depending on Neutron Irradiation

Original

Reliability Assessment of Nanoscale System on Chip Depending on Neutron Irradiation / Yang, Weitao; Li, Yang; Hu, Zhiliang; He, Chaohui; Cai, Jiale; Wu, Longsheng. - In: ELECTRONICS. - ISSN 2079-9292. - (2023).

Availability:

This version is available at: 11583/2978090 since: 2023-04-21T07:04:08Z

Publisher:

MDPI

Published

DOI:

Terms of use:

This article is made available under terms and conditions as specified in the corresponding bibliographic description in the repository

Publisher copyright

(Article begins on next page)

Reliability Assessment of Nanoscale System on Chip Depending on Neutron Irradiation

Weitao Yang^{a,b,c}, Yang Li^b, Zhiliang Hu^{b,c,d}, Chaohui He^b, Jiale Cai^f, Longsheng Wu^a

^aSchool of Microelectronics, Xidian University, Xi'an 710071, China

^bSchool of Nuclear Science & Technology, Xi'an Jiaotong University, Xi'an 710049, China

^cSpallation Neutron Source Science Center, Dongguan 523803, China

^dInstitute of High Energy Physics, Chinese Academy of Sciences (CAS), Beijing 100049, China

^eDipartimento di Automatica e Informatica, Politecnico di Torino, Torino 10129, Italy

^fDipartimento di Elettronica e Telecomunicazioni, Politecnico di Torino, Torino 10129, Italy

The atmospheric neutron poses a serious hazard to nanoscale electronics reliability. Spallation neutron irradiations on a nanoscale system on chip (SoC) were conducted applying the China Spallation Neutron Source (CSNS), and the results were compared and analyzed using Monte Carlo simulation. The contribution from thermal neutron on the SoC single event effect (SEE) was analyzed. Analysis indicated the SoC atmospheric neutron SEE vulnerability can be reduced by 44.4% if the thermal neutron was absorbed. The influences of the B and Hf elements on the SEEs were evaluated, too. It can be concluded that ^{10}B interacting with thermal neutron is the reason for thermal neutron inducing SEE in the SoC. Although the Hf element has no contribution to the 28 nm SoC atmospheric neutron SEE cross section, it increases the total dose risk 5 times during atmospheric neutron irradiation.

Keywords: Spallation Neutron; Monte Carlo; System on Chip; Thermal Neutron; Single Event Effect

1. Introduction

In 2001, Robert C. Baumann first reported ^{10}B interacting with thermal neutron is a dominant factor in soft errors for deep-submicron static random access memory with borophosphosilicate glass (BPSG) packages.^[1] Since then, advanced integrated circuit development makes the chip packages get rid of the BPSG package.^[2-3] The nanoscale electronics, however, even though the BPSG package is not available anymore, they have to face the risk from ^{10}B interacting with thermal neutron once again.^[4-7] The reason is ^{10}B still existing in the semiconductor contact and doping processes, and the rapidly developed semiconductor manufacturing technology pushes their supply voltages and single event effect (SEE) critical charges lower and lower.

In [6], C. Weulersse examined a variety of memories taking advantage of multi neutron sources and pointed out the related reliability problem. SEE, induced by ^{10}B in nanoscale memories via interacting with thermal neutron, is even close to that caused by high energy neutrons. In [8], the 65 nm microcontroller unit (MCU) without BPSG was irradiated with thermal and high energy neutrons, and the influence of ^{10}B on SEE was investigated. The results demonstrated that the contribution of ^{10}B interacting with thermal neutron even dominated the atmospheric neutron SEE in the device. Specifically, the SEE ratio induced by thermal and higher energy neutrons on the 65 nm MCU reached 1.89:1.^[8]

The 65 nm MCU test results signify that the interaction of ^{10}B with thermal neutron is still serious to advanced integrated chips. For the 28 nm SoC, besides the boron contamination, another is also introduced: the hafnium (Hf) element. Compared with boron (B), the neutron cross section with Hf is higher at several eV intervals. Fig.1 displays the neutron cross section spectrums of ^{10}B , ^{178}Hf , and ^{28}Si .^[9] It can be viewed the peak cross section of ^{178}Hf even achieves 10^5 barns. The cross sections of ^{178}Hf with thermal neutron are also higher than that of ^{28}Si by two orders of magnitudes. Another significant fact is that the B element exists in the

27 28 nm SoC as the contamination from manufacturing processes, while the Hf element is a
28 component of the metal gate in the 28 nm SoC. This process makes the 28 nm SoC atmospheric
29 neutron SEE evaluation become more complicated.

30 For the 28 nm SoC atmospheric neutron SEE, the first irradiation test has been conducted at
31 the China Spallation Neutron Source (CSNS)-BL09.^[10] In the irradiation, the neutron beam
32 hit the chip directly without any shield, and the neutron spectrum covered the thermal and
33 high energy neutrons. To explore the atmospheric neutron SEE on the 28 nm SoC further, the
34 second irradiation on the SoC was performed once more. But a 2 mm cadmium (Cd) slat was
35 used to absorb the thermal neutron before the irradiated chip compared with the previous. By
36 comparing the two irradiation results, thermal neutron's contribution to the 28 nm SoC can be
37 investigated. Meanwhile, the B and Hf elements' influence can be analyzed from the irradiation
38 and the Monte Carlo simulations.

39 2. Irradiation Tests

40 The actual atmospheric neutron SEE test is time-consuming, and the spectrum of the
41 spallation neutron source is the closest to the real one. Thus, it is considered the ideal
42 atmospheric neutron source.^[11] Scale-down manufacturing technology makes it urgent to
43 undertake more available atmospheric neutron SEE irradiation studies. The China spallation
44 neutron source was implemented in 2018 and made it come true to launch atmospheric neutron
45 SEE tests using a spallation neutron source in China.^[12] Fig.2 shows the calculated differential
46 flux of the neutron beam of CSNS (10⁹ of Peking ground).

47 Based on the CSNS-BL09, two SEE irradiation tests were conducted on the 28 nm SoC. In
48 [10], the first irradiation test was performed, and the SoC was irradiated by the neutron beam
49 directly without any shield. In the second irradiation test, that is the current work, a 2 mm
50 Cd slat was placed between the beam ejection stop and the tested chip to absorb thermal
51 neutrons. Fig.3 displays the neutron spectrum at the terminal with and without the 2 mm Cd slat
52 [8]. It can be seen that the 2 mm Cd slat absorbs the neutrons effectively whose energies are
53 below 0.5 eV.

54 The on-chip memory (OCM) block of the Xilinx Zynq-7000 SoC was tested in two
55 irradiations. The 64 kB data in the OCM were tested dynamically. The check pattern data,
56 0xA5A5A5A5, were written into the OCM addresses and read back by the SoC, and the SoC
57 compared the readback one with the check pattern data to determine whether a SEE took place.
58 The comparison results was moved to PC and refreshed in a terminal. It requires to compare
59 results with the first irradiation, where the normal condition is examined without any
60 mitigation techniques. Hence, the same condition is available in this effort.

61 In both irradiations, the test establishments are the same except the 2 mm Cd slat. A 2260B
62 programming DC power supplied the test board. The real-time current was monitored and
63 recorded by the remote host computer, and the possible single event latch-up was also
64 investigated. The host computer and the test board communicated through a universal serial
65 bus cable, and the running messages were recorded in real-time.

66 3. Results and Discussions

67 Four kinds of soft errors were detected in both irradiations, including the single bit upset
68 (SBU), dual cell upset (DCU), multi-cell upset (MCU), and single event functional interruption
69 (SEFI). No abnormal current was detected, which means no latch-up event emerged in the 28
70 nm SoC atmospheric neutron SEE irradiation tests. However, there are some differences
71 between the two irradiations in terms of SEE cross section. This discrepancy signifies thermal
72 neutron impacts the 28 nm SoC atmospheric neutron SEE.

73 3.1. The Detected Events

74 In the second irradiation, 19 events were detected. Table I lists the number of each type of
75 error. The number of SBU events is more than others. It is similar to that in the first irradiation.

76 During the second irradiation, the neutron flux above 1 MeV was about $6.85 \times 10^5 \text{ n} \cdot \text{cm}^{-2} \cdot \text{s}^{-1}$ and
 77 the corresponding fluence was $2.47 \times 10^{10} \text{ n} \cdot \text{cm}^{-2}$. Hence, the SBU cross section is
 78 $(5.26 \pm 0.26) \times 10^{-10} \text{ cm}^2$ and $(1.00 \pm 0.05) \times 10^{-15} \text{ cm}^2 \cdot \text{bit}^{-1}$ for the irradiation with few thermal
 79 neutrons.

80 Table I. The detected SEE in irradiation with few thermal neutrons

SBU	DCU	MCU	SEFI
13	2	2	2

81 Table II. The detected SEE in irradiation with thermal and high energy neutrons.^[10]

SBU	DCU	MCU	SEFI
21	4	2	5

82
 83 Table II presents the detected SEE in the first irradiation. It can be seen the number of SBU
 84 events is 21 in the irradiation, which is also more than others. In Table I and II, it is evident
 85 that SBU events dominate the detected soft errors in both irradiations.

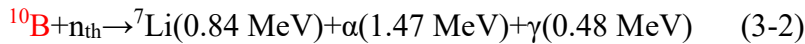
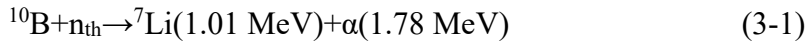
86 Table III presents the SBU cross sections in two irradiations. The neutron fluence of the
 87 second irradiation is $2.47 \times 10^{10} \text{ n} \cdot \text{cm}^{-2}$, higher than that of the first irradiation by 11.26%,
 88 however, the number of SBU event in the second irradiation is 13 instead of more than 21. This
 89 phenomenon implies thermal neutron has a contribution to the 28 nm SoC atmospheric neutron
 90 SEE. The discrepancy between the bit cross sections is $0.8 \times 10^{-15} \text{ cm}^2 \cdot \text{bit}^{-1}$. Since the critical
 91 difference between two irradiations is containing thermal neutron or not, it can be speculated
 92 thermal neutron causes the discrepancy. It attests the SEE sensitivity of the 28 nm SoC can be
 93 reduced by about 44.4% by shielding thermal neutron with a 2 mm Cd slat. All these
 94 demonstrate that risks from thermal neutron cannot be neglected, even though the nanoscale
 95 chips get rid of BPSG in packages.

96 Table III. The SBU cross sections in two irradiations.

Neutron Beam	Fluence 10^{10} cm^{-2}	SBU	Cross section 10^{-10} cm^2	Bit cross section $10^{-15} \text{ cm}^2 \cdot \text{bit}^{-1}$
CSNS-BL09 ^[10]	2.22	21	9.46 ± 0.47	1.80 ± 0.09
CSNS-BL09+2mm Cd	2.47	13	5.26 ± 0.26	1.00 ± 0.05

98 3.2. B Influence

99 The 65 nm MCU atmospheric neutron irradiation results indicated that the secondary
 100 particles from thermal neutrons interacting with ^{10}B could result in SEU on advanced electronic
 101 systems. Compared with the 65 nm memory cell, the SEU critical charge of the 28 nm memory
 102 cells is lower, and thermal neutron is easier to induce soft errors in the 28 nm process cells.



105 Formulas (3-1) and (3-2) describe the mechanisms of thermal neutron (n_{th}) reacting with ^{10}B .
 106 The probability of (3-1) is 6.3%, and that of (3-2) is 93.7%.^[13] It means the key of thermal
 107 neutron inducing SEE in the 28 nm SoC is $^7\text{Li}(0.84 \text{ MeV})$ and $\alpha(1.47 \text{ MeV})$ particles. They
 108 deposit energy in the sensitive volumes. Table IV shows the ranges in silicon and the linear
 109 energy transfers (LETs) of the two secondary particles.^[14] The ranges in silicon of $\alpha(1.47 \text{ MeV})$
 110 and $^7\text{Li}(0.84 \text{ MeV})$ are just 5 μm and 2.5 μm , which are much less than the thickness of the 28
 111 nm SoC from top passive layers to substrate's surface.^[15] This phenomenon preliminarily
 112 reveals that the B contamination exists inner the chip and approaches sensitive volumes of the

113 SoC. The SEE LET threshold of the 28 nm cell is approximately $0.50 \text{ MeV}\cdot\text{cm}^2\cdot\text{mg}^{-1}$.^[16] For
 114 ${}^7\text{Li}$ (0.84 MeV) and α (1.47 MeV), the LETs are $2.10 \text{ MeV}\cdot\text{cm}^2\cdot\text{mg}^{-1}$ and $1.15 \text{ MeV}\cdot\text{cm}^2\cdot\text{mg}^{-1}$,
 115 respectively. They are higher than the threshold, which means both secondary particles can
 116 induce SEE in 28nm SoC.

117 Table IV. The ranges and LETs of secondary particles of ${}^{10}\text{B}$ with the thermal neutron.

Rang in silicon/ μm		LET/ $\text{MeV}\cdot\text{cm}^2\cdot\text{mg}^{-1}$	
${}^7\text{Li}$ (0.84 MeV)	α (1.47 MeV)	${}^7\text{Li}$ (0.84 MeV)	α (1.47 MeV)
2.5	5	2.10	1.15

118 It is different from the 65 nm MCU, the Hf element also exists inner the 28 nm SoC, and the
 119 cross section of Hf with thermal neutron is even higher than that of silicon. Thus, it cannot
 120 conclude the difference is induced by ${}^{10}\text{B}$ directly.

121 3.3. Hf Influence

122 ${}^{10}\text{B}$, in the 28 nm SoC, interacts with thermal neutron inducing SEE, that mainly comes from
 123 the high probability of nuclear reaction. However, as Fig.4 displays, the primary interaction of
 124 thermal neutron and the Hf element is the (n, γ) reaction,^[9] and the γ rays usually results in
 125 total ionization dose rather than SEE in the device.^[17] Because the generated γ rays cannot
 126 cause SEE directly and have to interact with other atoms to produce secondary heavy ionization
 127 particles, this possibility is relatively low.

128 Compared with high energy neutrons, cross sections of ${}^{178}\text{Hf}$ interacting with the eV level
 129 neutrons even achieve 10^5 barns. In this case, whether the hafnium element contributes to 28
 130 nm SoC atmospheric neutron SEE, required to be comprehensively assessed.

131 In Fig.4, the peak's reaction of ${}^{178}\text{Hf}$ with several eV neutrons is elastic or (n, γ). As
 132 mentioned above, the contribution from (n, γ) reaction to induce SEE in 28nm SoC is rather
 133 low. Neutron in elastic interaction can transfer energy to hafnium atoms, it might increase the
 134 probability of causing SEE. The maximum transfer energy to the Hf atom from neutron can be
 135 calculated with the formula (3-3).^[18]

$$136 \quad E_t = \frac{4M_n M_t}{(M_n + M_t)^2} E_n \quad (3-3)$$

137 *E_t is the max energy transfer to Hf atom with keV, M_n is the mass of the neutron, which is*
 138 *1.67×10^{-27} kg, M_t is the Mass of Hf and it is 2.96×10^{-25} kg, and E_n is the energy of neutron*
 139 *with keV.*

140 The current work mainly discusses soft error in the 28 nm SoC induced by thermal neutron
 141 reacting with the boron and hafnium elements. As stated in Section 2, the neutron with energy
 142 less than 0.5 eV are absorbed by a 2 mm Cd slat. For the 0.5 eV neutron, the maximum
 143 transferred energy to Hf atom is about 0.01 eV. Meanwhile, considering the peak elastic cross
 144 section in Fig. 4, even though it extends the neutron energy to the rightmost peak, the
 145 corresponding max transferred energies are lower than 0.03 keV. Considering their LETs (the
 146 corresponding LETs are less than $0.50 \text{ MeV}\cdot\text{cm}^2\cdot\text{mg}^{-1}$), these are all impossible to lead to SEE
 147 on the SoC. It testifies the high cross section elastic interaction from Hf with thermal and eV
 148 neutrons does not affect 28nm SoC atmospheric neutron SEE.

149 Hence, it can be concluded the soft error difference between the two irradiations is mainly
 150 caused by ${}^{10}\text{B}$.

151 3.4. Monte Carlo Simulation

152 The cut cross section of the chip is investigated and captured, as shown in Fig. 5, the
 153 thickness and materials of the passive layers were obtained.^[10, 15] Meanwhile, the 28 nm High-
 154 k metal gate (HKMG) technology gate contains TiN(8 nm), HfO₂(10 nm), and SiON(1.2
 155 nm),^[19] and the ultra-thin SiON layer can also be an ultra-thin SiO₂ layer in the HKMG

156 technology.^[20] Relying on these effort and information, two Geant4 Monte Carlo simulation
 157 models were constructed to examine the Hf element's influence.^[21, 22] In Fig.6, the TiN and
 158 ultra-thin SiO₂ layers are considered only in the first model, while the TiN, HfO₂, and ultra-
 159 thin SiO₂ layers are considered simultaneously in the second model in Fig.7. Others are the
 160 same for the two simulation models.

161 The spectrum of neutron sources in the simulation is the same as in the first irradiation test,
 162 which includes thermal and high energy neutrons. The number of neutrons is 10⁷, and the
 163 surface area of the model is 10 μm×10 μm. 32×32 sensitive volumes (SVs) are placed, the size
 164 of the volume is 130 nm×130 nm×130 nm, and the critical charge is 0.18 fC. During the
 165 simulation, if the deposited energy in an SV overs the critical charge in an EventAction, which
 166 means an SEU emerged.

167 The number of the upset event in the cells and deposited doses in the ultra-thin SiO₂ layer
 168 were recorded in both simulations and shown in Table V. It can be seen the number of the upset
 169 event and the cross section are the same in both simulations. Still, the deposited dose in the
 170 ultra-thin SiO₂ layers differs by almost 5 times. The simulation results verify that the Hf
 171 element does not influence 28 nm SoC atmospheric neutron SEE. However, the existence of
 172 hafnium may increase the total dose risk during atmospheric neutron SEE irradiation. In Fig.4,
 173 the high (n, γ) cross section also underlines this possible outcomes, because more γ rays means
 174 more possible total ionization dose risk. And the simulation results is consistent with that. It
 175 suggests total dose risk monitoring is necessary in much more fluence atmospheric neutron
 176 SEE irradiation tests for the SoC.

177 Table V. The upset number and deposited doses in two simulations.

Upset number		Bit cross section/cm ² ·bit ⁻¹		Deposited Dose/rad	
First Model	Second Model	First Model	Second Model	First Model	Second Model
5	5	5×10 ⁻¹⁶	5×10 ⁻¹⁶	12.6	63.3

178 Up to now, we evaluated the 65 nm MCU and 28 nm SoC atmospheric neutron SEE
 179 depending on CSNS. In the future, more SEE irradiations and assessments will be explored
 180 further.

181 4. Conclusion

The 28 nm SoC was irradiated twice at CSNS-BL09. In the first irradiation, the spectre
 covered the thermal and high energy neutron, while thermal neutrons were shielded in the
 second. The differences in the results were analyzed. The discrepancy between the two
 irradiation tests is caused by ¹⁰B interacting with thermal neutron. If thermal neutron in the
 atmospheric environment is shielded by a 2 mm Cd slat, the 28 nm SoC SEE sensitivity can be
 decreased by 44.4%. The hafnium element does not influence the 28 nm SoC atmospheric
 neutron SEE, although it also has a high interaction cross section with thermal neutron. The
 evaluation illustrated attention should be paid to total dose hazard during the 28 nm SoC
 atmospheric neutron SEE irradiation, since the hafnium element increases the total dose risk.

182

183 Acknowledgment

184 Authors thank the engineers of CSNS-BL09.

185 Project supported by National Natural Science Foundation of China (Grant Nos. 11575138,
 186 11835006, 11690040, and 11690043)

187

188 References

189 1. R. C. Baumann and E. B. Smith, Neutron-induced 10B fission as a major source of soft

190 errors in high density SRAMs, 2001 *Microelectron. Reliab.* 41, 211.

191 2. N. Badodekar, Cypress white paper Document, no. 001-88889.

192 3. S. Kumar, S. Agarwal and J. P. Jung, Soft Error Issue and Importance of Low Alpha Solders
193 for Microelectronics Packaging, 2013 *Rev. Adv. Mater. Sci.* 34, 185-202.

194 4. Chen W, Yang H L and Guo X Q, et al., The research status and challenge of space radiation
195 physics and application, 2017 *Chin. Sci. Bull.* 62, 978-989.

196 5. T. Yamazaki, T. Kato, T. Uemura, et al., Origin analysis of thermal neutron soft error rate
197 at nanometer scale, 2015 *Journal of Vacuum Science & Technology B* 33, 020604.

198 6. C. Weulersse, S. Houssany and N. Guibbaud, et al., Contribution of Thermal Neutrons to
199 Soft Error Rate, 2018 *IEEE Trans. Nucl. Sci.* 65, 1851-1857.

200 7. Y. P. Fang and A. S. Oates, Thermal neutron-induced soft errors in advanced memory and
201 logic devices, 2014 *IEEE Trans. Device Mater. Rel.* 14, 583-586.

202 8. Z. Hu, W. Yang and Y. Li, et al., Atmospheric neutron single event effect in 65 nm
203 microcontroller units by using CSNS-BL09, 2019 *Acta Phys. Sin.* 68, 238502.

204 9. Brookhaven National Laboratory, National Nuclear Data
205 Center (NNDC), Evaluated Nuclear Data File (ENDF):
206 <https://www.nndc.bnl.gov/exfor/endl00.jsp>

207 10. W. Yang, Y. Li and Y. Li, et al., Atmospheric Neutron Single Event Effect Test on Xilinx
208 28nm System on Chip at CSNS-BL09. 2019 *Microelectron. Reliab.* 99, 119-124.

209 11. C. Andreani, R. Senesi and A. Paccagnella, et al., Fast neutron irradiation tests of flash
210 memories used in space environment at the ISIS spallation neutron source, 2018 *AIP Adv.*
211 8, 025013.

212 12. Y. Chen. China Spallation Neutron Source, 2011 *Bulletin of Chinese Academy of Sciences*,
213 26, 726-729.

214 13. Tian Y S, Hu Z L and Tong J F, et al., Design of beam shaping assembly based on 3.5 MeV radio-
215 frequency quadrupole proton accelerator for boron neutron capture therapy, 2018 *Acta Phys. Sin.*
216 67, 142801.

217 14. SRIM (2013). Particle Interactions with Matter [Online]. Available: <http://www.srim.org/>

218 15. W. Yang, Q. Yin and Y. Li, et al., Single-event effects induced by medium-energy protons in 28
219 nm system-on-chip, 2019 *Nucl. Sci. Tech.* 30, 151.

220 16. M. Amrbar, F. Irom and S. M. Guertin, et al., Heavy ion single event effects measurements of Xilinx
221 Zynq-7000 FPGA, 2015 *IEEE Radiat. Effects Data Workshop (REDW)*, Boston, MA, USA.

222 17. S. D. Mascioia, A. Menicuccia, G. Furano, et al., Towards defining a simplified procedure for COTS
223 system-on-chip TID testing, 2018, *Nucl. Eng. Tech.*, 50, 1298-1305.

224 18. C. Leroy, P. G. Rancoita, *Principles of Radiation Interaction in Matter and Detection (2nd Edition)*,
225 Word Scientific Publishing, 2009.

226 19. S. Uwe, C. S. Hwang, and H. Funakubo. Ferroelectricity in doped hafnium oxide: materials,
227 properties and devices. Woodhead Publishing, 2019.

228 20. M. Czernohorsky, K. Seidel and K. Kühnel, et al. High-K metal gate stacks with ultra-thin
229 interfacial layers formed by low temperature microwave-based plasma oxidation, 2017
230 *Microelectron. Eng.* 178, 262-265.

231 21. S. Agostinelli, J. Allison, and K. Amako et al., GEANT4-a simulation toolkit, 2003 *Nucl. Instrum.*
232 *Methods Phys. Res. A.* 506, 250-303.

233 22. W. Yang, Y. Li, W. Zhang, et al. Electron inducing soft errors in 28 nm system-on-Chip, 2020
234 *Radiation Effects and Defects in Solids*, 175, 745-754.